

Non-reversible perturbations of homoclinic snaking scenarios

Jürgen Knobloch

Institute of Mathematics,

Ilmenau University of Technology

Martin Vielitz

Institute of Mathematics,

Ilmenau University of Technology

Thomas Wagenknecht

Department of Applied Mathematics

University of Leeds

January 26, 2012

Abstract

Homoclinic snaking refers to the continuation curves of homoclinic orbits near a heteroclinic cycle, which connects an equilibrium and a periodic orbit in a reversible Hamiltonian system. We consider non-reversible perturbations of this situation and show analytically that such perturbations typically lead to either infinitely many closed continuation curves (isolas) or to two snaking continuation curves, which follow the primary sinusoidal continuation curves alternately (criss-cross snaking). These two scenarios are illustrated numerically with computations for perturbed versions of the Swift-Hohenberg equation.

1 Introduction

The term homoclinic snaking refers to the sinusoidally “snaking” continuation curves of homoclinic orbits, which exist near a heteroclinic cycle connecting an equilibrium E and a periodic orbit P , a so-called EtoP cycle. Homoclinic snaking has been observed in various examples of reversible Hamiltonian systems, [3, 11]. In this case homoclinic orbits to E are situated in a level set of the Hamiltonian and hence are typically robust, meaning that they will not be destroyed under (small) perturbations. Consequently, such orbits can be continued within a one-parameter family of differential equations, and the corresponding

continuation curves give rise to the characteristic snakes-and-ladder structure. As a specific example, let us consider the quadratic-cubic Swift-Hohenberg equation, given by

$$u_t = \mu u - (1 + \partial_x^2)^2 u + 2u^2 - u^3,$$

with μ as the bifurcation parameter. Stationary solutions of this equation satisfy the corresponding 4-th order ODE

$$u_{xxxx} = (\mu - 1)u - 2u_{xx} + 2u^2 - u^3, \quad (1.1)$$

and it is important to note that this equation is reversible, i.e. it is invariant under the symmetry $x \rightarrow -x$. In addition, Equation (1.1) conserves the first integral

$$F(u) = -\frac{1}{2}(\mu - 1)u^2 + u_x^2 - \frac{1}{2}u_{xx}^2 + u_x u_{xxx} - \frac{2}{3}u^3 + \frac{1}{4}u^4.$$

(Note that it is possible to introduce coordinates such that (1.1) can be written as a Hamiltonian system, see [11].)

It is well known that Equation (1.1) has a multitude of homoclinic solutions, which lie on one of a pair of bifurcation curves that snake between two parameter values, [3, 11]. The solutions along these snakes are symmetric with respect to the reversibility and resemble periodic patterns that are subjected to a localised amplitude modulation. The width of the periodic part increases when going up the snakes. In addition, the two snaking bifurcation curves are connected by branches of non-symmetric solutions, which emerge in pitchfork bifurcations near the folds along the snakes. This snakes-and-ladder structure and corresponding solutions are shown in Figure 1. All computational results in this paper have been obtained using AUTO, [5].

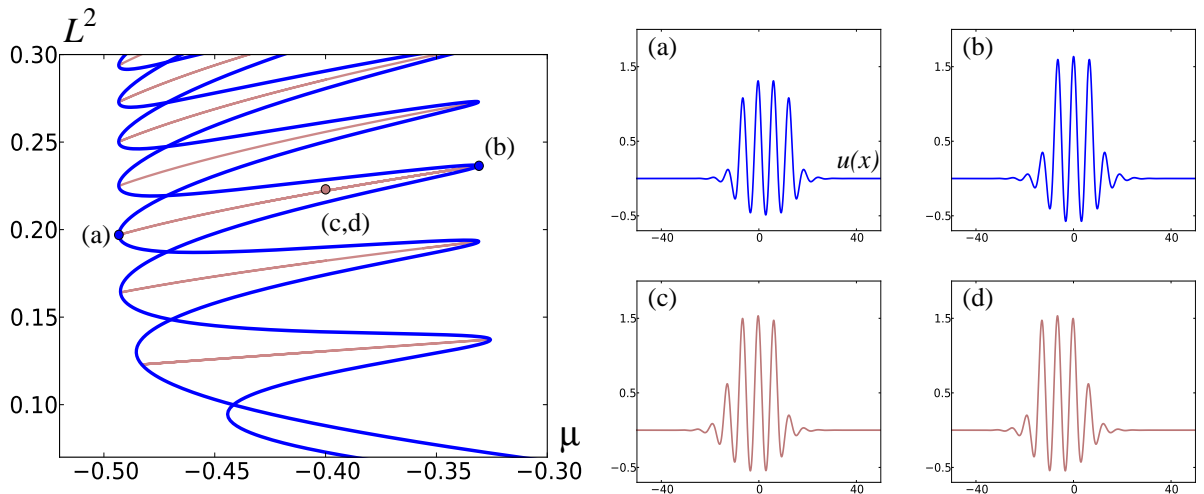


Figure 1: *Homoclinic snaking in the Swift-Hohenberg equation (1.1).*

In this paper we study non-reversible perturbations of such a snaking scenario. As explained above, homoclinic solutions will persist in symmetry-breaking perturbations of (1.1), which preserve the conservative character of the equation. But because the symmetry is broken, the pitchfork bifurcations will unfold, thus altering the overall bifurcation diagram. It turns out that two different scenarios are possible.

First, let us consider the equation

$$u_{xxxx} = (\mu - 1)u - 2u_{xx} + 2u^2 - u^3 + \lambda (3u_x u_{xx}^2 + u_x^2 u_{xxx}). \quad (1.2)$$

This ODE conserves the function

$$\hat{F}_\lambda(u) = F(u) + \lambda u_x^3 u_{xx},$$

but it is not reversible for $\lambda \neq 0$. Panel (a) in Figure 2 shows the bifurcation diagram for $\lambda = 0.3$. We see that the snakes-and-ladder structure breaks up into a family of stacked isolas. A similar result has been found in [2], where the authors consider perturbations that destroy both the symmetry and the conservative character of Equation (1.1).

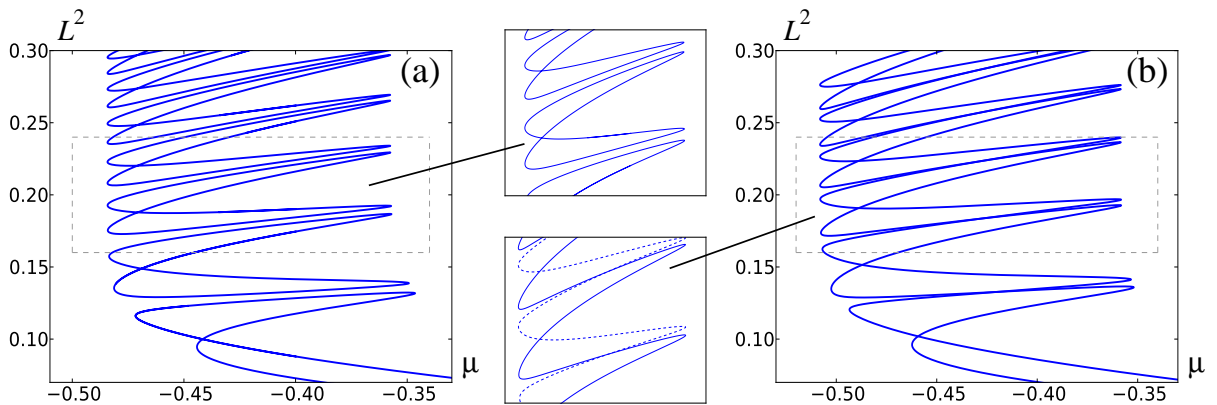


Figure 2: *Isolas of homoclinic solutions of Equation (1.2) with $\lambda = 0.3$ in panel (a) and criss-cross snaking of homoclinic solutions of Equation (1.3) with $\lambda = 0.3$ in panel (b). The middle part contains magnifications of parts of the diagrams as indicated.*

As a second example we choose the equation

$$u_{xxxx} = (\mu - 1)u - 2u_{xx} + 2u^2 - u^3 + 3\lambda u_x u_{xx}, \quad (1.3)$$

which has the first integral

$$\hat{F}_\lambda(u) = F(u) + \lambda u_x^3.$$

Again, the perturbation breaks the reversibility if $\lambda \neq 0$. We find that homoclinic solutions still lie on snakes in the bifurcation diagram, but in contrast to the situation for Equation (1.2), these snakes follow the complete snakes-and-ladder structure including the rungs, giving rise to what we call *criss-cross snaking*.

The aim of this paper is to show analytically that the numerical results represent the generic behaviour. Our analysis is based on the considerations in [1] and [7], and we consider a smooth family of differential equations

$$\dot{x} = f(x, \mu, \lambda), \quad x \in \mathbb{R}^4, \quad (\mu, \lambda) \in \mathbb{R}^2, \quad (1.4)$$

which we assume to be conservative for all values of the parameters, and reversible for $\lambda = 0$. As in the examples above, the parameter μ plays the role of the snaking parameter, and λ acts as perturbation parameter that breaks the reversibility, see Section 2 for details. We are interested in the continuation behaviour of one-homoclinic orbits to a hyperbolic equilibrium E , which exist within a small neighbourhood of a heteroclinic cycle connecting E and a periodic orbit P , called EtoP cycle. The periodic orbit is assumed to be hyperbolic within the corresponding level set of the first integral. Moreover, for $\lambda = 0$ we assume that both, E and P are symmetric, and so is the EtoP cycle.

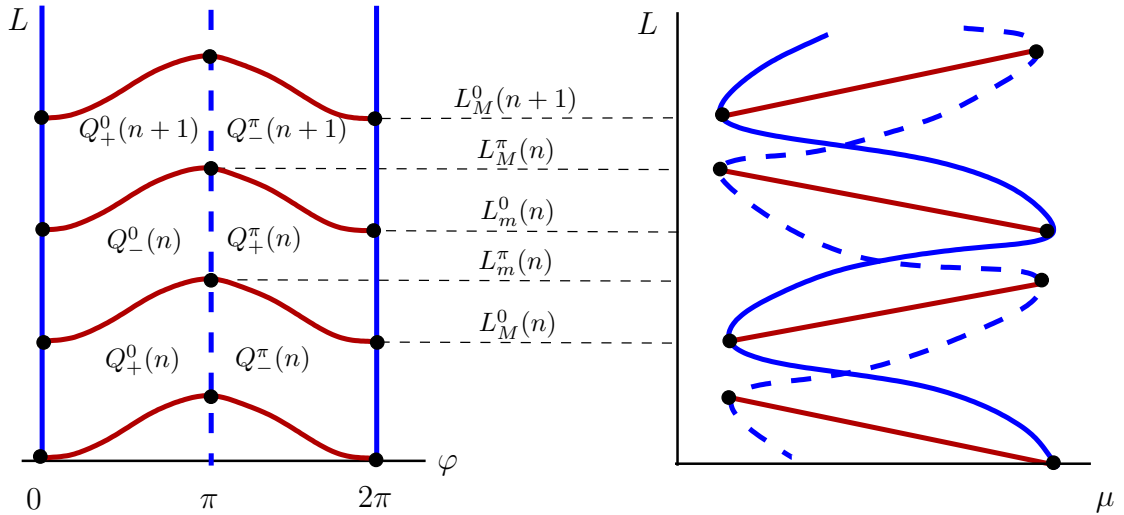


Figure 3: The left panel shows the zero-level set of Z_0 , and the left panel the snakes-and-ladder structure. Vertical lines on the left correspond to the snakes, and the horizontal curves correspond to the rungs in Figure 1. The level set is reflection-symmetric with respect to the line $\{\varphi = \pi\}$ and moreover 2π -periodic in φ , and so the outer vertical lines represent the same snaking curve. The lower index $+/-$ indicates that within the corresponding region $Q_{+/-}^{0/\pi}$ the function Z_0 is positive/negative.

Under our assumptions in Section 2 the continuation curves of homoclinic orbits for $\lambda = 0$ form a snakes-and-ladder structure as in Figure 1. This follows from the analysis in [1], where it was shown that the snaking behaviour is related to the behaviour of the intersection of the unstable manifold of E and the stable manifold of P . In particular, it turns out that the homoclinic orbits near the EtoP cycle are related to the zero-level set of a certain function Z_0 , see Section 2. This relation is illustrated in Figure 3, and these results form the starting

point for the analysis in the present paper. We will show that homoclinic orbits in the perturbed system correspond to the zero-level set of a symmetry-breaking perturbation Z of Z_0 . As a consequence, we find that two different scenarios are possible, depending on the behaviour of the perturbation Z . These scenarios are depicted in Figure 4.

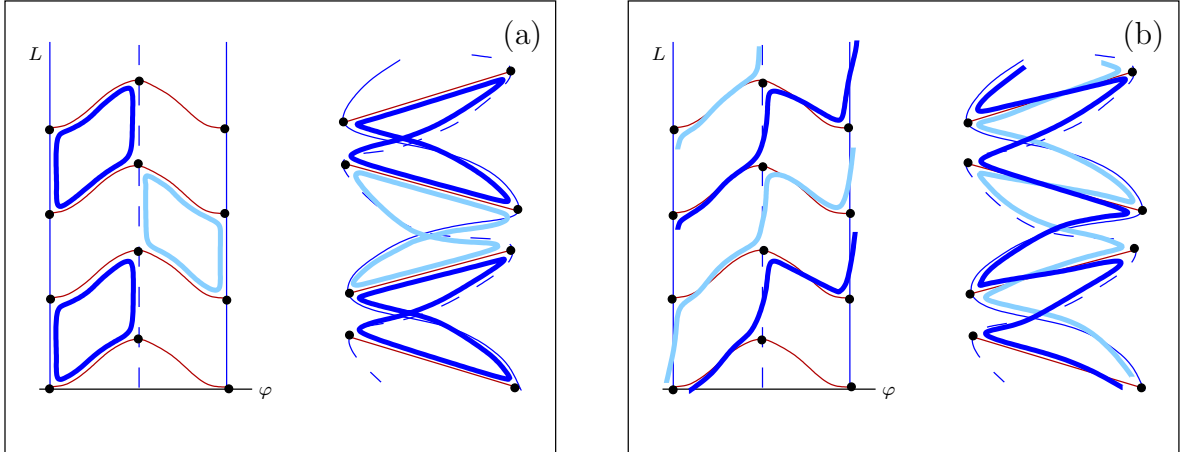


Figure 4: The left part in each panel shows the zero-level set of Z as a perturbation of the zero-level set of Z_0 . The right part in each panel shows the corresponding continuation curves for nearby homoclinic orbits as perturbations of the snaking scenario in Figure 2.

If the zero level-set of Z is a closed curve as in panel (a) of Figure 4, then the continuation curves are figure-eight shaped isolas, whereas the snaking-like curves in panel (b) are called *criss-cross snaking curves*. These curves follow alternately one of the original snaking curve, one of the branches of non-symmetric homoclinic orbits and further the other original snaking curve and so on.

We briefly want to discuss related work. In [2] perturbations of the Swift-Hohenberg equation that destroy both the reversibility and the first integral are studied numerically and similar effects of the perturbation on the continuation curves are observed. In the present paper we give an analytical reasoning for the observed behaviour under purely non-reversible perturbations. Our analysis is not restricted to the Swift-Hohenberg equation. As already mentioned, the approach in [1, 7] forms the basis of our considerations. In [1] the snaking behaviour of the unperturbed system is discussed in detail, whereas [7] analyses the behaviour of two-homoclinic orbits in the unperturbed system. It turns out that the corresponding determination equation for these orbits can also be seen as a perturbation of $Z_0 = 0$. Hence, our continuation analysis in Section 3 is inspired by those papers. In [4, 8] snaking in non-reversible, non-conservative systems is considered. The described snaking scenario is quite different from the present one. One reason for that is that in those systems the organising EtoP cycle has codimension one, in contrast to the present situation.

Finally we want to note that during the preparation of this article we have become aware of

work by Sandstede and Xu in [10], where in a similar way isolas and snaking continuation curves of homoclinic orbits in conservative (non-reversible) systems are found. Our emphasis however, lies on the consideration of non-reversible perturbations. This allows us to describe the corresponding isolas and snaking continuation curves against the background of the original snakes-and-ladder structure. In particular, this gives our notion of criss-cross snaking a real meaning.

The paper is organised as follows. In the following Section 2 we formulate the precise setup and our main result Theorem 1. Section 3 is devoted the proof of the main theorem. We conclude the paper with a short discussion.

2 Setup and main results

We consider Equation (1.4). Hypotheses (H1) and (H2) define the structure imposed on the vector field f :

Hypothesis (H1) *There exists a linear involution $R : \mathbb{R}^4 \rightarrow \mathbb{R}^4$, i.e. $R^2 = id$, such that*

$$f(Rx, \mu, 0) = -Rf(x, \mu, 0), \quad \forall x \in \mathbb{R}^4, \forall \mu \in \mathbb{R}.$$

Hypothesis (H1) states that for $\lambda = 0$ the vector field f is reversible. Recall that a solution $x(t)$ of a reversible differential equation is called symmetric, if the corresponding orbit is invariant under R , $R(\{x(t)\}) = \{x(t)\}$, or in other words if there is a τ such that $x(\tau) \in \text{Fix}(R)$, where $\text{Fix } R$ denotes the fixed space of R .

Hypothesis (H2) *Equation (1.4) has a smooth first integral $H : \mathbb{R}^4 \times \mathbb{R} \times \mathbb{R} \rightarrow \mathbb{R}$ with $H(Rx, \mu, 0) = H(x, \mu, 0)$.*

Next we introduce the equilibrium E and the periodic orbit P which are part of the EtoP cycle.

Hypothesis (H3) *There are compact intervals $J_\mu, J_\lambda \subset \mathbb{R}$ with nonempty interiors and $0 \in J_\lambda$ such that $E := \{x = 0\}$ is a hyperbolic equilibrium of (1.4) for all $(\mu, \lambda) \in J_\mu \times J_\lambda$.*

Obviously, for $\lambda = 0$ the hyperbolic equilibrium E is symmetric, $R(E) = E$. This implies that the corresponding stable and unstable manifolds are R -images of each other, $R(W^s(E, \mu, 0)) = W^u(E, \mu, 0)$, and it also means that the dimensions of these manifolds coincide. Consequently, for all $(\mu, \lambda) \in J_\mu \times J_\lambda$ it holds $\dim W^s(E, \mu, \lambda) = \dim W^u(E, \mu, \lambda) = 2$. Moreover, the dimension of $\text{Fix}(R)$ is half of the space dimension, i.e. $\dim \text{Fix}(R) = 2$.

Hypothesis (H4) For all $(\mu, \lambda) \in J_\mu \times J_\lambda$, Equation (1.4) has a periodic orbit $P = \gamma(t, \mu, \lambda)$ with minimal period 2π , which satisfies the following:

- (i) The family $\gamma(t, \mu, \lambda)$ depends smoothly on (μ, λ) .
- (ii) $\gamma(0, \mu, 0) \in \text{Fix}(R)$.
- (iii) $H(\gamma(t, \mu, \lambda), \mu, \lambda) = H(E, \mu, \lambda) = 0$ and $D_x H(\gamma(t, \mu, \lambda), \mu, \lambda) \neq 0$ for all $t \in \mathbb{R}$.
- (iv) $\gamma(t, \mu, \lambda)$ has, in addition to 1, Floquet multipliers $e^{2\pi\alpha^s(\mu, \lambda)} < 1 < e^{2\pi\alpha^u(\mu, \lambda)}$.

Due to Hypothesis (H4)(ii) the periodic orbit $P = \gamma(t, \mu, 0)$ is symmetric. This implies that also $\gamma(\pi, \mu, 0) \in \text{Fix}(R)$, and that the Floquet exponents satisfy $\alpha^s(\mu, 0) = -\alpha^u(\mu, 0)$. Hypothesis (H4)(iv) implies that restricted to the zero level set of H , the orbit P is hyperbolic with two-dimensional stable and unstable manifolds $W^s(P, \mu, \lambda)$ and $W^u(P, \mu, \lambda)$, respectively. Moreover, due to Hypothesis (H4)(iv) and the compactness of $J_\mu \times J_\lambda$ the Floquet exponents are bounded away from zero.

In order to characterise the EtoP cycle and its behaviour when changing μ we introduce within the level set $\{H = 0\}$ near P local coordinates (v^c, v^s, v^u) with the following properties:

$$\begin{aligned} W_{loc}^s(P, \mu, \lambda) &= \{v^u = 0\}, \\ W_{loc}^u(P, \mu, \lambda) &= \{v^s = 0\}, \\ P &= \{v^s = 0, v^u = 0\}. \end{aligned}$$

We exploit the following lemma to establish these coordinates, cf. [1]:

Lemma 2.1 Assume Hypotheses (H1), (H2) and (H4) are met, then there is a smooth change of coordinates locally near P such that $\dot{x} = f(x, \mu, \lambda)$ becomes

$$\begin{aligned} \dot{v}^c &= 1 + A^c(v, \mu, \lambda)v^s v^u, \\ \dot{v}^s &= (\alpha^s(\mu, \lambda) + A^s(v, \mu, \lambda))v^s, \\ \dot{v}^u &= (\alpha^u(\mu, \lambda) + A^u(v, \mu, \lambda))v^u, \end{aligned} \tag{2.1}$$

where $v = (v^c, v^s, v^u) \in S^1 \times I \times I$ and A^c, A^s, A^u are some smooth functions in v and μ, λ with

$$A^i(0, \mu, \lambda) = 0, \quad i = c, s, u, \quad \forall \mu \in J_\mu, \forall \lambda \in J_\lambda.$$

Moreover, for $\lambda = 0$ the vector field in (2.1) is reversible, and the reverser R acts in these coordinates as

$$R(v^c, v^s, v^u) = (-v^c, v^u, v^s). \tag{2.2}$$

Since the variable v^c is considered as $v^c \in S^1 := \mathbb{R}/\sim_{2\pi}$, and $x \sim_{2\pi} y \Leftrightarrow x = y \pmod{2\pi}$, Equation (2.2) yields that the fixed space $\text{Fix}(R)$ of R within the level set of P is given by

$$\text{Fix}(R) \cap \{H = 0\} = \{(0, v^s, v^s)\} \cup \{(\pi, v^s, v^s)\}.$$

Now let $\delta > 0$ be a sufficiently small constant and $I := [-\delta, \delta]$. We define sections

$$\Sigma^{\text{in}} := S^1 \times \{v^s = \delta\} \times I, \quad \Sigma^{\text{out}} := S^1 \times I \times \{v^u = \delta\},$$

cf. Figure 5. Note that these sections are R -images of each other.

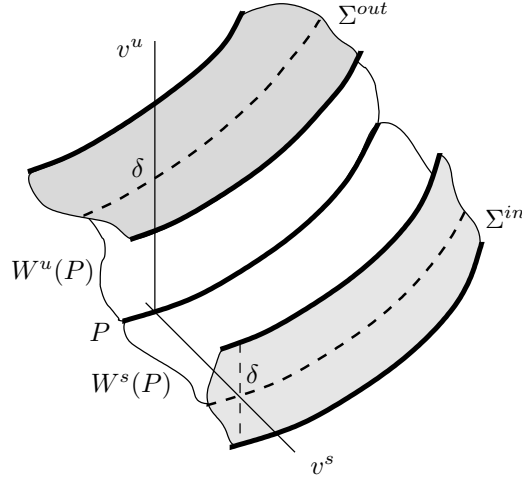


Figure 5: *The cross-sections Σ^{in} and Σ^{out} .*

We finally define the EtoP cycle, which lies in the intersection of the stable and unstable manifolds of E and P . For this we denote the strong stable and strong unstable fibers of P with base point $\gamma(\varphi, \mu, \lambda)$ by $W^{ss}(\gamma(\varphi, \mu, \lambda), \mu, \lambda)$ and $W^{uu}(\gamma(\varphi, \mu, \lambda), \mu, \lambda)$, respectively, and define, cf. [1],

$$\begin{aligned} \Gamma^{\text{out}} &:= \{(\varphi, \mu) \in S^1 \times J_\mu : W^s(E, \mu, 0) \cap W^{uu}(\gamma(\varphi, \mu, 0), \mu, 0) \cap \Sigma^{\text{out}} \neq \emptyset\}, \\ \Gamma_\lambda^{\text{in}} &:= \{(\varphi, \mu) \in S^1 \times J_\mu : W^u(E, \mu, \lambda) \cap W^{ss}(\gamma(\varphi, \mu, \lambda), \mu, \lambda) \cap \Sigma^{\text{in}} \neq \emptyset\}. \end{aligned}$$

Note that due to the first equation in (2.1) the v^c -coordinate of $\gamma(\varphi, \mu, \lambda)$ is equal to φ . Furthermore we observe that in the reversible system with $\lambda = 0$, the sets Γ^{out} and Γ_0^{in} are R -images of each other. In the end the symmetry breaking perturbation will be realised by the assumption that Γ^{out} and $\Gamma_{\lambda \neq 0}^{\text{in}}$ are no longer R -images of each other, cf. Hypotheses (H6)–(H8) below.

As in [1], we assume that both $\Gamma_\lambda^{\text{in}}$ and Γ^{out} are the graph of a function.

Hypothesis (H5) *The sets Γ^{out} and $\Gamma_\lambda^{\text{in}}$ are graphs of smooth functions $z_{\text{out}} : S^1 \rightarrow \mathring{J}_\mu$ and $z_{\text{in}}(\cdot, \lambda) : S^1 \rightarrow \mathring{J}_\mu$, respectively, where $\lambda \in J_\lambda$, and \mathring{J}_μ is the interior of J_μ . The function z_{in} depends smoothly on λ . Moreover $z'_{\text{out}}(\varphi) = 0$ if and only if $\varphi \in \{\ell_m, \ell_M\}$ and $z''_{\text{out}}(\ell_m), z''_{\text{out}}(\ell_M) \neq 0$, and $z_{\text{out}}(\ell_m) < z_{\text{out}}(\ell_M)$.*

In other words, z_{out} has precisely two critical points, one minimum taken at ℓ_m and one maximum taken at ℓ_M , which are both non-degenerate. Figure 6 illustrates the situation.

Note that we assume that z_{out} does not depend on the perturbation parameter λ . This restriction is not necessary for our analysis and is only used to simplify our notation.

As a direct consequence of the reversibility at $\lambda = 0$, we find that

$$z_{in}(\varphi, 0) = z_{out}(-\varphi). \quad (2.3)$$

Next we state assumptions on the stable and unstable manifolds of E :

Hypothesis (H6) *There exist an open neighbourhood $U_{\Gamma^{out}}$ of Γ^{out} in $S^1 \times J_\mu$, an $\epsilon > 0$ and a smooth function $g^s : U_{\Gamma^{out}} \times J_\lambda \rightarrow I$ such that for all $\lambda \in J_\lambda$*

$$\{(\varphi, v^s, \delta) \in W^s(E, \mu, \lambda) \cap \Sigma^{out} : |v^s| < \epsilon, (\varphi, \mu) \in U_{\Gamma^{out}}\} = \{(\varphi, g^s(\varphi, \mu, \lambda), \delta) : (\varphi, \mu) \in U_{\Gamma^{out}}\}.$$

Moreover there exists a constant $b > 0$ such that $|D_\mu g^s(\varphi, \mu, \lambda)| > b > 0$ for all (φ, μ, λ) .

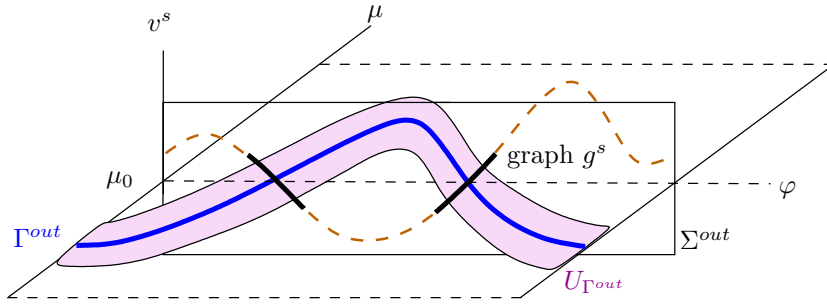


Figure 6: The set Γ^{out} within its open neighbourhood $U_{\Gamma^{out}}$. The graph of g^s is drawn for $\mu = \mu_0$. The dashed lines indicate a possible continuation of the g^s outside of $U_{\Gamma^{out}}$.

Hypothesis (H7) *There exist an open set $U_{\Gamma^{in}}$ in $S^1 \times J_\mu$, which is for all $\lambda \in J_\lambda$ an open neighbourhood of Γ_λ^{in} , an $\epsilon > 0$ and a smooth function $h^u : U_{\Gamma^{in}} \times J_\lambda \rightarrow I$ such that for all $\lambda \in J_\lambda$*

$$\{(\varphi, \delta, v^u) \in W^u(E, \mu, \lambda) \cap \Sigma^{in} : |v^u| < \epsilon, (\varphi, \mu) \in U_{\Gamma^{in}}\} = \{(\varphi, \delta, h^u(\varphi, \mu, \lambda)) : (\varphi, \mu) \in U_{\Gamma^{in}}\}.$$

Reversibility implies

$$h^u(\varphi, \mu, 0) = g^s(-\varphi, \mu, 0).$$

Therefore, due to Hypothesis (H6) for all (φ, μ, λ) , λ sufficiently small it holds

$$|D_\mu h^u(\varphi, \mu, \lambda)| > b > 0. \quad (2.4)$$

Note that the zeros of g^s do not depend on λ , which corresponds to the assumption that Γ^{out} is independent of λ . The Hypotheses (H5), (H6) or (H5), (H7) imply that

$$g^s(\varphi, \mu, \lambda) = 0 \Leftrightarrow \mu = z_{out}(\varphi) \quad \text{or} \quad h^u(\varphi, \mu, \lambda) = 0 \Leftrightarrow \mu = z_{in}(\varphi, \lambda), \quad (2.5)$$

respectively.

It is proved in [1] that due to Hypotheses (H3)-(H6) homoclinic snaking as depicted in Figure 1 occurs in the unperturbed system with $\lambda = 0$. More precisely, there it was shown that, restricted to a neighbourhood of the EtoP cycle, one-homoclinic orbits to E are determined by an equation

$$Z_0(\varphi, L) = 0 \quad (2.6)$$

in the following manner: There is a mapping $\mu_0^* : S^1 \times \mathbb{R}^+ \rightarrow I_\mu$ such that $\dot{x} = f(x, \mu, 0)$ has a corresponding homoclinic orbit that spends time $2L$ between Σ^{in} and Σ^{out} if and only if there is some φ such that (φ, L) solves (2.6) and $\mu = \mu_0^*(\varphi, L)$. The zeros of Z_0 are depicted in the left panel in Figure 3, whereas the right panel in Figure 3 displays the set $\{(\mu_0^*(\varphi, L), L) : Z_0(\varphi, L) = 0\}$. In the present paper we derive the function Z_0 in Section 3.1.

In order to define the non-reversible perturbations we consider the difference $z_{in}(-\varphi, \lambda) - z_{out}(\varphi)$. Exploiting (2.3) we define the smooth function $\hat{z}(\varphi, \lambda)$ by:

$$\lambda \hat{z}(\varphi, \lambda) := z_{in}(-\varphi, \lambda) - z_{out}(\varphi). \quad (2.7)$$

The vector field f is non-reversible for $\lambda \neq 0$, if $\hat{z}(\varphi, \lambda) \neq 0$. We distinguish the following two cases:

Hypothesis (H8) $\hat{z}(\ell_M, 0) \neq 0$, $\hat{z}(\ell_m, 0) \neq 0$ and $\text{sgn}(\hat{z}(\ell_M, 0)) = \text{sgn}(\hat{z}(\ell_m, 0))$.

Hypothesis (H9) $\hat{z}(\ell_M, 0) \neq 0$, $\hat{z}(\ell_m, 0) \neq 0$ and $\text{sgn}(\hat{z}(\ell_M, 0)) \neq \text{sgn}(\hat{z}(\ell_m, 0))$.

Theorem 1 *Assume Hypotheses (H1) - (H7) and either (H8) or (H9). There exist positive constants L^0 and λ^0 , and there are functions $\mu_\lambda^* : S^1 \times \mathbb{R}^+ \rightarrow I_\mu$ such that for $|\lambda| < \lambda^0$ Equation (1.4) has a homoclinic orbit that spends the time $2L$ between the cross-sections Σ^{in} and Σ^{out} , if (μ, L) lies on a continuation curve $(\mu_\lambda^*(\varphi_\lambda(s), L_\lambda(s)), L_\lambda(s))$ distinguished by the following: The mapping $(\varphi, L) \mapsto (\mu_0^*(\varphi, L), L)$ maps the zero-level set of Z_0 onto the original snakes-and-ladder structure. Further, if $\lambda \neq 0$, and*

- (i) *Hypothesis (H8) is met: There is an $N_0 > 0$ such that for all $n > N_0$ there are closed curves $(\varphi_{\lambda,n}^0(s), L_{\lambda,n}^0(s))$ and $(\varphi_{\lambda,n}^\pi(s), L_{\lambda,n}^\pi(s))$. These curves are close to the boundaries $\partial Q_+^0(n)$ and $\partial Q_+^\pi(n)$ or $\partial Q_-^0(n)$ and $\partial Q_-^\pi(n)$, respectively, cf. Figure 3 and Figure 4, panel (a).*

(ii) *Hypothesis (H9) is met: There are two continuation curves $(\varphi_{\lambda,i}(s), L_{\lambda,i}(s))$, $i = 1, 2$. Both curves are close to the zero-level set of Z_0 . Further, the $L_{\lambda,i}$ are unbounded. Approaching a saddle point of Z_0 these curves turn alternately to the left or to the right, cf. Figure 4, panel (b).*

In either instance the union of these curves converges in the Hausdorff distance to $\{Z_0 = 0\}$, as λ tends to zero.

If the curves $(\varphi_{\lambda,n}^{0/\pi}(s), L_{\lambda,n}^{0/\pi}(s))$ approach a saddle point of Z_0 they turn always in the same direction.

The corresponding continuation curves $(\mu_\lambda^*(\varphi_{\lambda,n}^{0/\pi}(s), L_{\lambda,n}^{0/\pi}(s))$, $n > N_0$ or $(\mu_\lambda^*(\varphi_{\lambda,i}(s), L_{\lambda,i}(s))$, $i = 1, 2$, respectively are shown on the right of each panel of Figure 4. If Hypothesis (H8) is met the continuation curves form isolas for $\lambda \neq 0$. If, on the other hand Hypothesis (H9) is met the homoclinic orbits can be continued along criss-cross snaking curves.

3 Continuation analysis

This section is devoted the proof of Theorem 1. As a first step we derive the determination equation for one-homoclinic orbits to E in a vicinity of the primary EtoP cycle. For this we assume Hypotheses (H1) - (H7). Afterwards we discuss the determination equation under the additional Hypothesis (H8) or (H9), respectively.

3.1 The determination equation for one-homoclinic orbits

The addressed homoclinic solutions of (1.4) correspond to solutions $v(\cdot, \mu, \lambda)$ of (2.1) with

$$v(-L, \mu, \lambda) \in \Sigma^{in} \cap W^u(E, \mu, \lambda) \quad \text{and} \quad v(L, \mu, \lambda) \in \Sigma^{out} \cap W^s(E, \mu, \lambda),$$

for some $L \gg 1$. The next theorem, which describes the solutions of (2.1) in a vicinity of the periodic orbit P , is due to [1, 9].

Theorem 2 *Consider (2.1) under the assumptions of Lemma 2.1. There exist positive constants L_0, δ_0, λ_0 such that for all L, λ, δ with*

$$|\lambda| < \lambda_0, \quad 0 < \delta < \delta_0, \quad L > L_0$$

equation (2.1) has a unique solution $v(\cdot, \varphi, \mu, \lambda) = (v^c(\cdot, \varphi, \mu, \lambda), v^s(\cdot, \varphi, \mu, \lambda), v^u(\cdot, \varphi, \mu, \lambda))$ with

$$v^s(-L, \varphi, \mu, \lambda) \in \Sigma^{in}, \quad v^c(0, \varphi, \mu, \lambda) = \varphi, \quad v^u(L, \varphi, \mu, \lambda) \in \Sigma^{out}.$$

Moreover there exists a positive constant η such that the following estimates hold:

$$v(-L, \varphi, \mu, \lambda) = (-L + \varphi + O(e^{-\eta L}), \delta, a^u e^{-2\alpha^u L} + O(e^{-(2\alpha^u + \eta)L})), \quad (3.1)$$

$$v(L, \varphi, \mu, \lambda) = (L + \varphi + O(e^{-\eta L}), a^s e^{2\alpha^s L} + O(e^{(2\alpha^s - \eta)L}), \delta), \quad (3.2)$$

where $a^{s/u} = a^{s/u}(L, \delta, \mu, \lambda)$ are smooth, bounded functions. For $\lambda = 0$ the reverser acts on the solution v as

$$v(L, -\varphi, \mu, 0) = Rv(-L, \varphi, \mu, 0).$$

Furthermore, if the vector field in (2.1) is C^{k+1} -smooth, then the derivatives of this solution are given by

$$D_{\nu_1, \dots, \nu_l} v(-L, \varphi, \mu, \lambda) = D_{\nu_1, \dots, \nu_l} (-L + \varphi, \delta, a^u e^{-2\alpha^u L}) + (O(e^{-\eta L}), 0, O(e^{-(2\alpha^u + \eta)L})),$$

$$D_{\nu_1, \dots, \nu_l} v(L, \varphi, \mu, \lambda) = D_{\nu_1, \dots, \nu_l} (L + \varphi, a^s e^{2\alpha^s L}, \delta) + (O(e^{-\eta L}), O(e^{(2\alpha^s - \eta)L}), 0),$$

where $\nu_i = L, \mu, \lambda, \varphi$, $i = 1, \dots, l$, $l \in \{1, \dots, k\}$.

Note that due to Hypothesis (H4) the Floquet exponents $\alpha^{s/u}$ depend smoothly on μ and λ .

According to Theorem 2 we find one-homoclinic orbits to E by solving

$$\begin{aligned} v^u(-L, \varphi, \mu, \lambda) &= h^u(v^c(-L, \varphi, \mu, \lambda), \mu, \lambda), \\ v^s(L, \varphi, \mu, \lambda) &= g^s(v^c(L, \varphi, \mu, \lambda), \mu, \lambda). \end{aligned} \quad (3.3)$$

Using the representations (3.1) and (3.2) these equations can be written as

$$a^u e^{-2\alpha^u(\mu, \lambda)L} (1 + O(e^{-\eta L})) = h^u(-L + \varphi + O(e^{-\eta L}), \mu, \lambda), \quad (3.4)$$

$$a^s e^{2\alpha^s(\mu, \lambda)L} (1 + O(e^{-\eta L})) = g^s(L + \varphi + O(e^{-\eta L}), \mu, \lambda). \quad (3.5)$$

Equation (2.5) implies that $h^u(\varphi, z_{in}(\varphi, \lambda), \lambda) \equiv 0$ and $g^s(\varphi, z_{out}(\varphi), \lambda) \equiv 0$. With that said equations (3.4) and (3.5) can be solved for

$$\begin{aligned} \mu &= \mu_{in}(L, \varphi, \lambda) = z_{in}(-L + \varphi, \lambda) + e_{in}(L, \varphi, \lambda), \\ \mu &= \mu_{out}(L, \varphi, \lambda) = z_{out}(L + \varphi) + e_{out}(L, \varphi, \lambda), \end{aligned} \quad (3.6)$$

respectively, where $e_{in}(L, \varphi, 0) = O(e^{-\eta L})$ and $e_{out}(L, \varphi, 0) = O(e^{-\eta L})$. For a more detailed analysis we refer to [1, Section 4 and Section 5.2]. Further, the reversibility implies that $\mu_{out}(L, \varphi, 0) = \mu_{in}(L, -\varphi, 0)$, and hence

$$e_{out}(L, \varphi, 0) = e_{in}(L, -\varphi, 0). \quad (3.7)$$

Lemma 3.1 $e_{in/out}(L, \varphi, \lambda) = e_{in/out}(L, \varphi, 0) + \lambda O(e^{-\eta L})$, uniformly in λ .

The proof of this lemma will be given at the end of this subsection.

Summarising, a homoclinic solution to E exists at the parameter value μ , if both (3.4) and (3.5) are satisfied. Thus the determination equation for homoclinic orbits to E reads:

$$Z(L, \varphi, \lambda) := \mu_{out}(L, \varphi, \lambda) - \mu_{in}(L, \varphi, \lambda) = 0.$$

Using the representation (3.6) together with (2.7), Lemma 3.1 and (3.7), the function Z can be written as

$$\begin{aligned} Z(L, \varphi, \lambda) = & z_{out}(L + \varphi) - z_{out}(L - \varphi) + e_{out}(L, \varphi, 0) - e_{out}(L, -\varphi, 0) \\ & - \lambda(\hat{z}(L - \varphi, \lambda) + O(e^{-\eta L})). \end{aligned}$$

With $Z_0(L, \varphi) := Z(L, \varphi, 0)$ the determination equation reads

$$Z(L, \varphi, \lambda) = Z_0(L, \varphi) - \lambda(\hat{z}(L - \varphi, \lambda) + O(e^{-\eta L})) = 0. \quad (3.8)$$

Note that $Z_0 = 0$ is the determination equation of homoclinic orbits of the unperturbed system, so that the snaking behaviour of the unperturbed system is also represented in this equation. The zero level set of Z_0 was investigated in [1], where it was shown that it looks as illustrated in Figure 3 and that in particular $Z_0(L, 0) = Z_0(L, \pi) = 0$. These lines correspond to the snaking curves of symmetric homoclinic orbits. Further it was shown that the critical points of Z_0 in $\{Z_0 = 0\}$ are given by $(\varphi, L_i^\varphi(n))$ with $i \in \{m, M\}$ and $\varphi \in \{0, \pi\}$ and are related to the critical points of z_{out} by

$$L_i^\varphi(n) = \ell_i - \varphi + 2\pi n + O(e^{-\eta n}), \quad n \in \mathbb{N}, n \gg 1. \quad (3.9)$$

These points are saddle points of Z_0 and correspond to pitchfork points, where non-symmetric homoclinic orbits bifurcate from symmetric homoclinic orbits. The branches of these non-symmetric homoclinic orbits correspond to the vertical lines in the left panel of Figure 3.

Proof of Lemma 3.1. We show that $D_\lambda e_{in}(L, \varphi, \lambda) = O(e^{-\eta L})$. To this end we consider, cf (3.6),

$$D_\lambda \mu_{in}(L, \varphi, \lambda) = D_\lambda z_{in}(-L + \varphi, \lambda) + D_\lambda e_{in}(L, \varphi, \lambda). \quad (3.10)$$

Because μ_{in} solves the first equation in (3.3) we find for the left-hand side of (3.10)

$$D_\lambda \mu_{in}(L, \varphi, \lambda) = \frac{N(L, \varphi, \mu_{in}, \lambda)}{M(L, \varphi, \mu_{in}, \lambda)},$$

where

$$\begin{aligned} N(L, \varphi, \mu_{in}, \lambda) := & D_\lambda v^u(-L, \varphi, \mu_{in}, \lambda) - D_\varphi h^u(v^c(-L, \varphi, \mu_{in}, \lambda), \mu_{in}, \lambda) \cdot D_\lambda v^c(-L, \varphi, \mu_{in}, \lambda) \\ & - D_\lambda h^u(v^c(-L, \varphi, \mu_{in}, \lambda), \mu_{in}, \lambda), \\ M(L, \varphi, \mu_{in}, \lambda) := & -D_\mu v^u(-L, \varphi, \mu_{in}, \lambda) + D_\mu h^u(v^c(-L, \varphi, \mu_{in}, \lambda), \mu_{in}, \lambda) \\ & + D_\varphi h^u(v^c(-L, \varphi, \mu_{in}, \lambda), \mu_{in}, \lambda) \cdot D_\mu v^c(-L, \varphi, \mu_{in}, \lambda). \end{aligned}$$

The estimates given in Theorem 2 yield

$$D_\lambda \mu_{in}(L, \varphi, \lambda) = \frac{O(e^{-\eta L}) - D_\lambda h^u(-L + \varphi + O(e^{-\eta L}), \mu_{in}, \lambda)}{D_\mu h^u(-L + \varphi + O(e^{-\eta L}), \mu_{in}, \lambda) + O(e^{-\eta L})}.$$

Note that due to (2.4) the denominator is bounded away from zero. Note further that for arbitrarily large L the points $(-L + \varphi, \mu_{in}(L, \varphi, \lambda))$ belong to a compact subset of $U_{\Gamma in}$. Hence

$$D_\lambda \mu_{in}(L, \varphi, \lambda) = O(e^{-\eta L}) - \frac{D_\lambda h^u(-L + \varphi, \mu_{in}, \lambda)}{D_\mu h^u(-L + \varphi, \mu_{in}, \lambda) + O(e^{-\eta L})}. \quad (3.11)$$

Next we consider $D_\lambda z_{in}(-L + \varphi, \lambda)$ and recall that $h^u(-L + \varphi, z_{in}(-L + \varphi, \lambda), \lambda) = 0$, see (2.5). Therefore

$$D_\lambda z_{in}(-L + \varphi, \lambda) = -\frac{D_\lambda h^u(-L + \varphi, \mu_{in} - e_{in}(L, \varphi, \lambda), \lambda)}{D_\mu h^u(-L + \varphi, \mu_{in} - e_{in}(L, \varphi, \lambda), \lambda)}.$$

Using $e_{in}(L, \varphi, \lambda) = O(e^{-\eta L})$ we find

$$D_\lambda z_{in}(-L + \varphi, \lambda) = O(e^{-\eta L}) - \frac{D_\lambda h^u(-L + \varphi, \mu_{in}, \lambda)}{D_\mu h^u(-L + \varphi, \mu_{in}, \lambda) + O(e^{-\eta L})}. \quad (3.12)$$

Combining (3.11) and (3.12) yields $D_\lambda \mu_{in}(L, \varphi, \lambda) - D_\lambda z_{in}(-L + \varphi, \lambda) = O(e^{-\eta L})$. Together with (3.10) this proves the lemma. \blacksquare

3.2 Continuation in the perturbed system

We solve the determination equation (3.8) near the zero-level set of Z_0 . This level set consists of points $P_i^\varphi(n)$,

$$P_i^\varphi(n) = (\varphi, L_i^\varphi(n)), \quad i \in \{m, M\}, \quad \varphi \in \{0, \pi\},$$

and curve segments connecting these points as shown in Figure 3.

Using the implicit function theorem we show that (3.8) can be (uniquely) solved near compact parts of the line segments. These parts can be extended into small neighbourhoods of the adjacent points $P_i^\varphi(n)$.

Therefore, a small neighbourhood of $P_i^\varphi(n)$ contains four points $P_i^\varphi(n; j; \lambda)$, $j \in \{l, r, b, t\}$, belonging to four mutual disjoint curves gained by applying the implicit function theorem, cf. Figure 7. Which of these points can be connected by solution sets of (3.8) depends on the Hypotheses (H8) and (H9). By means of these hypotheses we define ‘‘barriers’’ which separate solution sets of (3.8). Figure 7 shows the alignment of those barriers which are related to Hypothesis (H8), panel (a) or Hypothesis (H9), panel (b), respectively, together with the complete solution sets of (3.8).

In order to verify that the corresponding points $P_i^\varphi(n; j; \lambda)$, $j \in \{l, r, b, t\}$ can really be connected we use arguments based on the Morse Lemma.

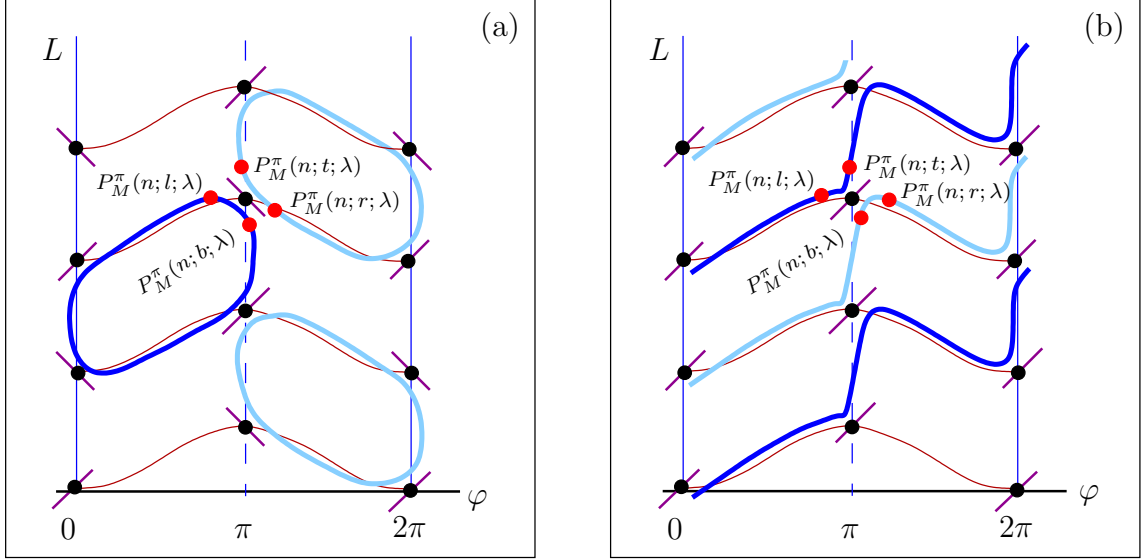


Figure 7: *Barriers together with the corresponding solution sets of (3.8).*

3.2.1 Continuation near curve segments

We use the implicit function theorem to solve the determination equation along the curve segments of the zero level-set of Z_0 . Let $(\hat{L}, \hat{\varphi}) \in \{Z_0 = 0\}$, $(\hat{L}, \hat{\varphi}) \neq P_i^\varphi(n)$. We write $L = \hat{L} + l$ and $\varphi = \hat{\varphi} + \psi$ and consider

$$\tilde{Z}(l, \psi, \lambda) := Z(\hat{L} + l, \hat{\varphi} + \psi, \lambda) = 0.$$

Note that $\tilde{Z}(0, 0, 0) = Z_0(\hat{L}, \hat{\varphi}) = 0$. Next we show that $D_{(l, \psi)} \tilde{Z}(0, 0, 0) = D_{(l, \psi)} Z_0(\hat{L}, \hat{\varphi}) \neq 0$: We first note that

$$D_{(l, \psi)} Z_0(L, \varphi) = (z'_{out}(L + \varphi) - z'_{out}(L - \varphi) + O(e^{-\eta L}), z'_{out}(L + \varphi) + z'_{out}(L - \varphi) + O(e^{-\eta L})).$$

Hence, $D_{(l, \psi)} Z_0(L, \varphi) = 0$ is equivalent to

$$z'_{out}(L - \varphi) + O(e^{-\eta L}) = 0, \quad z'_{out}(L + \varphi) + O(e^{-\eta L}) = 0.$$

Discussing these equations it turns out that, cf. [7],

$$D_{(l, \psi)} Z_0(L, \varphi) = 0 \quad \Leftrightarrow \quad (L, \varphi) = P_i^\varphi(n), \quad i \in \{m, M\}, \quad \varphi \in \{0, \pi\}, \quad n > N_0. \quad (3.13)$$

Altogether this shows that $\tilde{Z} = 0$ can be solved near $(\hat{L}, \hat{\varphi}, 0)$ either for $l = l_*(\psi, \lambda)$ or for $\psi = \psi_*(l, \lambda)$. Note that these functions also depend on $(\hat{L}, \hat{\varphi})$, but we suppress this in the notation. Moreover, there is a $\lambda_1 > 0$ such that all those l_* or ψ_* are defined for $|\lambda| < \lambda_1$. This is obvious if \hat{L} is taken from a compact interval. However, due to the structure of $D_{(l, \psi)} \tilde{Z}(0, 0, 0)$, it remains also true for arbitrarily large \hat{L} .

Varying $(\hat{L}, \hat{\varphi}, 0)$ along a curve segment between neighbours $P_{i_1}^{\varphi_1}(n_1)$ and $P_{i_2}^{\varphi_2}(n_2)$ shows that there is a smooth solution curve of $Z = 0$ connecting arbitrarily small neighbourhoods of $P_{i_1}^{\varphi_1}(n_1)$ and $P_{i_2}^{\varphi_2}(n_2)$.

3.2.2 Definition of barriers

We show that there are certain line segments attached to the critical points of Z_0 in its zero-level set, along which there are no solution of the determination equation $Z = 0$.

Let $i \in \{m, M\}$ and $\varphi \in \{0, \pi\}$. Recall that $Z_0(L_i^\varphi, \varphi) = 0$. Hence, in accordance with (3.8) and (3.9) we find

$$Z(L_i^\varphi(n), \varphi, \lambda) = -\lambda(\hat{z}(l_i, \lambda) + O(e^{-\eta n})). \quad (3.14)$$

Therefore, for sufficiently large n

$$\text{sgn } Z(L_i^\varphi(n), \varphi, \lambda) = -\text{sgn } \lambda \cdot \text{sgn } \hat{z}(l_i, \lambda). \quad (3.15)$$

Let $\hat{z}(l_i, 0) > 0$, and let $\lambda < 0$. Then $Z(L_i^\varphi(n), \varphi, \lambda) > 0$, and according to (3.8) also $Z(L, \varphi, \lambda) > 0$ for $(L, \varphi) \in Q_+^{0/\pi}$ adjacent to $P_i^\varphi(n)$, (L, φ) close to $P_i^\varphi(n)$. In this case we define barriers $B_i^\varphi(n)$, $i \in \{m, M\}$ on which Z is definitely different from zero by

$$B_m^\varphi(n) := P_m^\varphi(n) + s(1, 1), \quad B_M^\varphi(n) := P_M^\varphi(n) + s(-1, 1), \quad |s| \text{ small.}$$

The described situation is depicted in Figure 8. In a similar way we proceed for $\lambda \hat{z}(l_i, 0) > 0$.

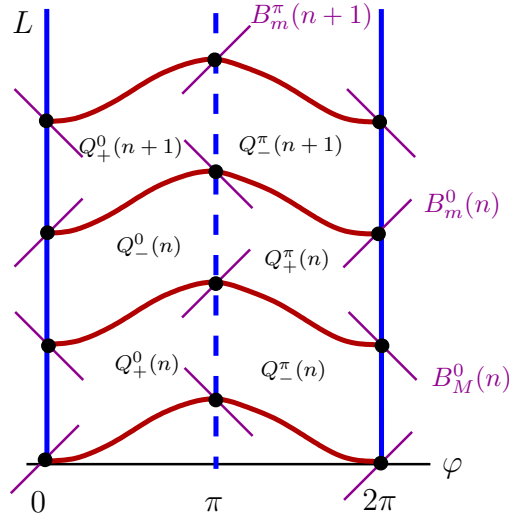


Figure 8: Bifurcation diagram with the (purple) barrier lines $B_i^{0/\pi}(n)$ in the vicinity of the critical points of Z_0 in $\{Z_0 = 0\}$. The diagram is drawn for the situation given by Hypothesis (H8), more precisely for $\lambda \text{sgn}(\hat{z}(l_i, 0)) < 0$, $i = m, M$. Along the purple lines the function Z is strictly positive. Hence no homoclinic solution exists along the barrier lines.

3.2.3 Joining of different solution branches of $Z = 0$

In Section 3.2.1 we have determined solution branches of $Z = 0$ connecting small neighbourhoods of adjacent saddle points of Z_0 . Here we discuss how near such a saddle point

$P_i^\varphi(n)$ appropriate branches can be joined. In doing so we exploit that $Z(\cdot, \cdot, \lambda)$ has a saddle point $\mathcal{P}_i^\varphi(n; \lambda)$ close to $P_i^\varphi(n)$. This saddle point does not belong to the zero-level set of Z . However, $Z(\mathcal{P}_i^\varphi(n; \lambda), \lambda)$ tends to zero as λ tends to zero. Consequently, near $\mathcal{P}_i^\varphi(n; \lambda)$ there are two curve segments belonging to the zero-level set of Z . Both curves connect two of the solution branches established in Section 3.2.1, respectively.

In order to make this procedure rigorous we consider the following. The points $P_i^\varphi(n)$, $i \in \{m, M\}$, $\varphi \in \{0, \pi\}$, $n > N_0$, are saddle points of Z_0 :

$$D_{(L, \varphi)}^2 Z_0(L_i^\varphi(n), \varphi) = \begin{pmatrix} 0 & 2z''_{out}(l_i) + O(e^{-\eta n}) \\ 2z''_{out}(l_i) + O(e^{-\eta n}) & 0 \end{pmatrix}.$$

The zeros in this representation follow from $Z_0(L, 0) = Z_0(L, \pi) = 0$ and the reflection symmetry of $\{Z_0 = 0\}$, cf. also [1, 7]. By Hypothesis (H5) the Hessian $D_{(L, \varphi)}^2 Z_0(L_i^\varphi(n), \varphi)$ is nondegenerate. Therefore, near $P_i^\varphi(n)$ the equation $D_{(L, \varphi)} Z(L, \varphi, \lambda) = 0$ can be solved for $(L, \varphi) = (L, \varphi)(\lambda) =: \mathcal{P}_i^\varphi(n; \lambda)$. It follows immediately that $D_{(L, \varphi)}^2 Z(\mathcal{P}_i^\varphi(n; \lambda), \lambda)$ is nondegenerate.

By similar arguments as in Section 3.2.1 there is a $\lambda_2 < \lambda_1$ such that for $i \in \{m, M\}$, $\varphi \in \{0, \pi\}$ and all $n > N_0$ the points $\mathcal{P}_i^\varphi(n; \lambda)$ are defined for all $|\lambda| < \lambda_2$.

Lemma 3.2 $Z(\mathcal{P}_i^\varphi(n; \lambda), \lambda) \neq 0$, for $\lambda \neq 0$.

Proof. First we note that $Z(\mathcal{P}_i^\varphi(n; 0), 0) = Z_0(P_i^\varphi(n)) = 0$. Further, due to (3.13) and (3.14) we find

$$\left. \frac{d}{d\lambda} Z(\mathcal{P}_i^\varphi(n; \lambda), \lambda) \right|_{\lambda=0} = -\hat{z}(l_i, 0) + O(e^{-\eta n}).$$

Due to Hypotheses (H8) or (H9), respectively, this derivative is different from zero. ■

However,

$$\lim_{\lambda \rightarrow 0} Z(\mathcal{P}_i^\varphi(n; \lambda), \lambda) = Z_0(P_i^\varphi(n)) = 0.$$

Due to the Morse Lemma, [6] there is an $r > 0$ such that on the ball $K(\mathcal{P}_i^\varphi(n; \lambda), r)$ centred at $\mathcal{P}_i^\varphi(n; \lambda)$ with radius r , there is a smooth coordinate transformation $(x, y) = \mathcal{T}(\varphi, L)$ such that

$$Z(\varphi, L, \lambda) = Z(\mathcal{P}_i^\varphi(n; \lambda), \lambda) + D_{(L, \varphi)}^2 Z(\mathcal{P}_i^\varphi(n; \lambda), \lambda)((x, y), (x, y)).$$

Indeed, inspecting the proof of the Morse Lemma we find that there is a $\lambda_0 < \lambda_2$ such that r can be chosen independently from $i \in \{m, M\}$, $\varphi \in \{0, \pi\}$, $n > N_0$ and $|\lambda| < \lambda_0$.

Note that within $K(\mathcal{P}_i^\varphi(n; \lambda), r)$ all level sets of Z , except the one related to $\mathcal{P}_i^\varphi(n; \lambda)$, consist of a pair of curves each running from boundary to boundary of $K(\mathcal{P}_i^\varphi(n; \lambda), r)$.

Now choose λ sufficiently small, such that the points $P_i^\varphi(n; j; \lambda)$, $j \in \{l, r, b, t\}$ are in $K(\mathcal{P}_i^\varphi(n; \lambda), r)$. Then, each two of these points are connected by a smooth curve belonging

to the zero-level set of Z . Which of these points are connected in this way depends on the alignment of the barriers defined in Section 3.2.2.

Isolas: Assume Hypothesis (H8), and more specifically that $\hat{z}(\ell_M, 0) > 0$ and $\hat{z}(\ell_m, 0) > 0$. If $\lambda < 0$, the barriers are aligned as depicted in Figure 8. The corresponding continuation curves form isolas. These are depicted in Figure 7, panel (a). Roughly speaking these isolas surround regions $Q_-^i(n)$. If λ has the opposite sign those isolas surround regions $Q_+^i(n)$. As λ tends to zero, the isolas tend to $\{Z = 0\}$ in the Hausdorff distance.

Criss-cross snaking: Assume Hypothesis (H9), and more specifically that $\hat{z}(\ell_M, 0) < 0$, $\hat{z}(\ell_m, 0) > 0$, and assume $\lambda < 0$. For the points $P_m^\varphi(n)$ we just repeat the discussion following (3.15). It turns out that the corresponding barriers take the form $B_m^\varphi(n) := P_m^\varphi(n) + s(1, 1)$. For the barriers at $P_M^\varphi(n)$ a similar discussion yields the same alignment, $B_M^\varphi(n) := P_M^\varphi(n) + s(1, 1)$. This situation together with the corresponding criss-cross snaking curves is depicted in Figure 7, panel (b). If λ changes sign the criss-cross snaking curves become descending. As λ tends to zero the criss-cross snaking curves tend to $\{Z = 0\}$ in the Hausdorff distance.

4 Discussion

In this paper we have studied symmetry-breaking perturbations of homoclinic snaking scenarios. Adapting the approach in [1, 7] we could show that the continuation curves of homoclinic orbits in the perturbed system are generically either isolas or criss-cross snakes.

It is an interesting question if and how the two different bifurcation scenarios can be transformed into one another. In order to address this problem we consider a homotopy between the two examples considered in the introduction, which is given by

$$u_{xxxx} = \mu u - u - 2u_{xx} + 2u^2 - u^3 + \lambda (\tau (3u_x u_{xx}^2 + u_x^2 u_{xxx}) + (1 - \tau) (3u_x u_{xx})), \quad (4.1)$$

where as above $\lambda = 0.3$. If $\tau = 1$, then homoclinic solutions to the equilibrium $E = 0$ lie on isolas in the bifurcation diagram, while for $\tau = 0$ the system exhibits criss-cross snaking, compare with Figure 2.

Our numerical studies show that isolas and criss-cross snaking persist for $\tau \approx 1$ and $\tau \approx 0$, respectively, and that a transition occurs for $\tau \in [0.1, 0.2]$. This transition process is illustrated in Figure 9.

If we decrease the parameter from $\tau = 0.2$, then figure-eight type isolas at the lower end of the bifurcation diagram, i.e. those corresponding to solutions with a narrow middle part, merge to form a larger isola. This occurs in a transcritical bifurcation near the fold on the left, as indicated in the panels containing magnified parts of panel (c) in Figure 9.

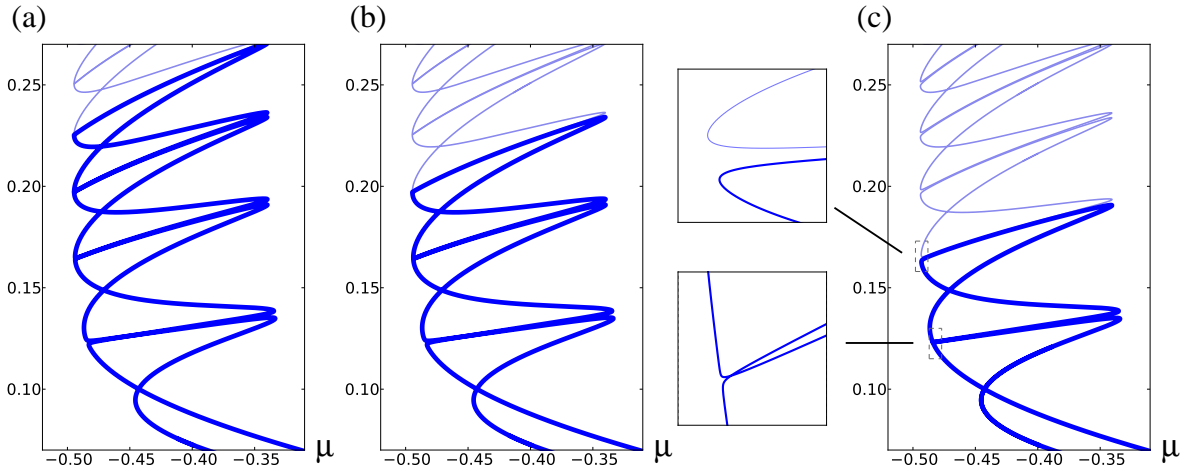


Figure 9: *Break-up of criss-cross snaking into isolas in Equation (4.1). The dark bold curves show large isolas, while the lighter curves are separate isolas of figure-eight type. The values of the homotopy parameter are $\tau = 0.109$ in (a), $\tau = 0.11$ in (b) and $\tau = 0.15$ in (c).*

The process continues if τ is decreased further, see panels (a) and (b). The values of the homotopy parameter τ at which further figure-eight isolas merge with the large isola at the bottom of the bifurcation diagram seem to converge to a finite value, such that at $\tau = 0.1$ the whole criss-cross snaking structure appears to be recovered. (The numerical results are necessarily incomplete, since only a finite part of the whole structure can be computed.)

These results are clearly different from the generic behaviour established in our analysis. Indeed, since the homotopy connects the two different scenarios in hypotheses (H9) and (H8), there must be a value τ_0 such that $\hat{z}(\ell_M, \lambda) = 0$ or $\hat{z}(\ell_m, \lambda) = 0$. The numerical results suggest that $\tau_0 \approx 0.1$, and it will be interesting to investigate an unfolding of this situation in detail. This is beyond our scope here, and we will explore this in future work.

References

- [1] M. Beck, J. Knobloch, D. J. B. Lloyd, B. Sandstede and T. Wagenknecht. Snakes, ladders, and isolas of localised patterns. *SIAM J. Math. Anal.* **41** (2009) 936–972.
- [2] J. Burke, S. M. Houghton and E. Knobloch. Swift–Hohenberg equation with broken reflection symmetry. *Phys. Rev. E* **80** (2009) 036202.
- [3] J. Burke and E. Knobloch, Snakes and ladders: localized states in the Swift-Hohenberg equation. *Phys. Lett. A* **360** (2007) 681–688.
- [4] A. R. Champneys, V. Kirk, E. Knobloch, B. E. Oldeman and J. D. M. Rademacher.

- Unfolding a tangent equilibrium-to-periodic heteroclinic cycle. *SIAM J. Appl. Dyn. Syst.* **8** (2009) 1261–1304.
- [5] E. J. Doedel and B. E. Oldeman. *AUTO-07P: Continuation and bifurcation software for ordinary differential equations*. Technical Report, Concordia University, 2009.
- [6] M. Golubitsky and V. Guillemin *Stable mappings and their singularities*. Springer 1973.
- [7] J. Knobloch, D.J.B. Lloyd, B. Sandstede, T. Wagenknecht. Isolas of 2-pulses in homoclinic snaking scenarios. *J. Dynamics and Differential Equations* **23** (2011) 93–114.
- [8] J. Knobloch, T. Rieß and M. Vielitz. Nonreversible Homoclinic Snaking. *Dynamical Systems* **26** (2011) 335–365.
- [9] M. Krupa, B. Sandstede and P. Szmolyan. Fast and slow waves in the FitzHugh-Nagumo equation. *J. Differ. Equations* **133** (1997) 49–97.
- [10] B. Sandstede and Y. Xu. Snakes and isolas in non-reversible conservative systems. *Preprint 2011*.
- [11] P. D. Woods and A. R. Champneys, Heteroclinic tangles and homoclinic snaking in the unfolding of a degenerate reversible Hamiltonian-Hopf bifurcation. *Physica D* **129** (1999) 147–170.